Benchmark Computations of Laminar Flow Around a Cylinder

M. Schäfer[a] and S. Turek[b]

(With support by F. Durst[a], E. Krause[c] and R. Rannacher[b])

[a]Lehrstuhl für Strömungsmechanik, Universität Erlangen-Nürnberg
Cauerstr. 4, D-91058 Erlangen, Germany
[b]Institut für Angewandte Mathematik, Universität Heidelberg
INF 294, D-69120 Heidelberg, Germany
[c]Aerodynamisches Institut, RWTH Aachen
Wüllnerstr. zw. 5 u. 7, D-52062 Aachen, Germany

SUMMARY

An overview of benchmark computations for 2D and 3D laminar flows around a cylinder is given, which have been defined for a comparison of different solution approaches for the incompressible Navier-Stokes equations developed within the Priority Research Programme. The exact definitions of the benchmarks are recapitulated and the numerical schemes and computers employed by the various participating groups are summarized. A detailed evaluation of the results provided is given, also including a comparison with a reference experiment. The principal purpose of the benchmarks is discussed and some general conclusions which can be drawn from the results are formulated.

1. INTRODUCTION

Under the DFG Priority Research Program "Flow Simulation on High Performance Computers" solution methods for various flow problems have been developed with considerable success. In many cases, the computing times are still very long and, because of a lack of storage capacity and insufficient resolution, the agreement between the computed results and experimental data is - even for laminar flows - only qualitative in nature. If numerical solutions are to play a similar role to wind tunnels, they have to provide the same accuracy as measurements, in particular in the prediction of the overall forces.

Several new techniques such as "unstructured grids", "multigrid", "operator splitting", "domain decomposition" and "mesh adaptation" have been used in order to improve the performance of numerical methods. To facilitate the comparison of these solution approaches, a set of benchmark problems has been defined and all participants of the Priority Research Program working on incompressible flows have been invited to submit their solutions. This paper presents the results of these computations contributed by altogether 17 research groups, 10 from within of the Priority Research Program and 7 from outside. The major purpose of the benchmark is to establish, whether constructive conclusions can be drawn from a comparison of these results so that the solutions can be improved. It is not the aim to come to the conclusion that a particular solution A is better than another solution B; the intention is rather to determine whether and why certain

approaches are superior to others. The benchmark is particularly meant to stimulate future work.

In the first step, only incompressible laminar test cases in two and three dimensions have been selected which are not too complicated, but still contain most difficulties representative of industrial flows in this regime. In particular, characteristic quantities such as drag and lift coefficients have to be computed in order to measure the ability to produce quantitatively accurate results. This benchmark aims to develop objective criteria for the evaluation of the different algorithmic approaches. For this purpose, the participants have been asked to submit a fairly complete account of their computational results together with detailed information about the discretization and solution methods used. As a result it should be possible, at least for this particular class of flows, to distinguish between "efficient" and "less efficient" solution approaches. After this benchmark has been proved to be successful it will be extended to include also certain turbulent and compressible flows.

It is particularly hoped that this benchmark will provide the basis for reaching decisive answers to the following questions which are currently the subject of controversial discussion:

1. Is it possible to calculate incompressible (laminar) flows accurately and efficiently by methods based on explicitly advancing momentum?

2. Can one construct an efficient solver for incompressible flow without employing multigrid components, at least for the pressure Poisson equation?

3. Do conventional finite difference methods have advantages over new finite element or finite volume techniques?

4. Can steady-state solutions be efficiently computed by pseudo-time-stepping techniques?

5. Is a low-order treatment of the convective term competitive, possibly for smaller Reynolds numbers?

6. What is the "best" strategy for time stepping: fully coupled iteration or operator splitting (pressure correction scheme)?

7. Does it pay to use higher order discretizations in space or time?

8. What is the potential of using unstructured grids?

9. What is the potential of a posteriori grid adaptation and time step selection in flow computations?

10. What is the "best" approach to handle the nonlinearity: quasi-Newton iteration or nonlinear multigrid?

These questions appear to be of vital importance in the construction of efficient and reliable solvers, particularly in three space dimensions. Everybody who is extensively consuming computer resources for numerical flow simulation should be interested.

The authors have tried their best in presenting and evaluating the contributed results in as much detail as possible and hope that all participants of the benchmark will find themselves correctly quoted.

2. DEFINITION OF TEST CASES

This section gives a brief summary of the definitions of the test cases for the benchmark computations, including precise definitions of the quantities which had to be computed and also some additional instructions which were given to the participants.

2.1 Fluid Properties

The fluid properties are identical for all test cases. An incompressible Newtonian fluid is considered for which the conservation equations of mass and momentum are

$$\frac{\partial U_i}{\partial x_i} = 0$$

$$\rho \frac{\partial U_i}{\partial t} + \rho \frac{\partial}{\partial x_j}\left(U_j U_i\right) = \rho \nu \frac{\partial}{\partial x_j}\left(\frac{\partial U_i}{\partial x_j} + \frac{\partial U_j}{\partial x_i}\right) - \frac{\partial P}{\partial x_i}$$

The notations are time t, cartesian coordinates $(x_1, x_2, x_3) = (x, y, z)$, pressure P and velocity components $(U_1, U_2, U_3) = (U, V, W)$. The kinematic viscosity is defined as $\nu = 10^{-3}\,\mathrm{m}^2/\mathrm{s}$, and the fluid density is $\rho = 1.0\,\mathrm{kg}/\mathrm{m}^3$.

2.2 2D Cases

For the 2D test cases the flow around a cylinder with circular cross–section is considered. The geometry and the boundary conditions are indicated in Fig. 1. For all test cases the

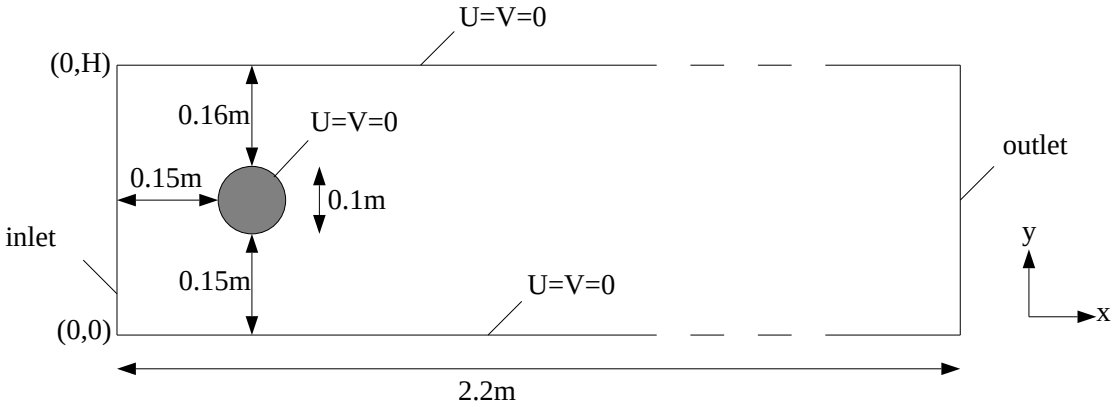

Figure 1: *Geometry of 2D test cases with boundary conditions*

outflow condition can be chosen by the user.

Some definitions are introduced to specify the values which have to be computed. $H = 0.41\,\mathrm{m}$ is the channel height and $D = 0.1\,\mathrm{m}$ is the cylinder diameter. The Reynolds number is defined by $Re = \overline{U}D/\nu$ with the mean velocity $\overline{U}(t) = 2U(0, H/2, t)/3$. The drag

and lift forces are

$$F_D = \int_S (\rho\nu \frac{\partial v_t}{\partial n} n_y - P n_x)\, dS \quad , \quad F_L = -\int_S (\rho\nu \frac{\partial v_t}{\partial n} n_x + P n_y)\, dS$$

with the following notations: circle S, normal vector n on S with x-component n_x and y-component n_y, tangential velocity v_t on S and tangent vector $t = (n_y, -n_x)$. The drag and lift coefficients are

$$c_D = \frac{2F_w}{\rho \overline{U}^2 D} \quad , \quad c_L = \frac{2F_a}{\rho \overline{U}^2 D}$$

The Strouhal number is defined as $St = Df/\overline{U}$, where f is the frequency of separation. The length of recirculation is $L_a = x_r - x_e$, where $x_e = 0.25$ is the x-coordinate of the end of the cylinder and x_r is the x-coordinate of the end of the recirculation area. As a further reference value the pressure difference $\Delta P = \Delta P(t) = P(x_a, y_a, t) - P(x_e, y_e, t)$ is defined, with the front and end point of the cylinder $(x_a, y_a) = (0.15, 0.2)$ and $(x_e, y_e) = (0.25, 0.2)$, respectively.

a) Test case 2D-1 (steady):

The inflow condition is

$$U(0, y) = 4U_m y(H - y)/H^2,\ V = 0$$

with $U_m = 0.3\,\mathrm{m/s}$, yielding the Reynolds number $Re = 20$. The following quantities should be computed: drag coefficient c_D, lift coefficient c_L, length of recirculation zone L_a and pressure difference ΔP.

b) Test case 2D-2 (unsteady):

The inflow condition is

$$U(0, y, t) = 4U_m y(H - y)/H^2,\ V = 0$$

with $U_m = 1.5\,\mathrm{m/s}$, yielding the Reynolds number $Re = 100$. The following quantities should be computed: drag coefficient c_D, lift coefficient c_L and pressure difference ΔP as functions of time for <u>one</u> period $[t_0, t_0 + 1/f]$ (with $f = f(c_L)$), maximum drag coefficient c_{Dmax}, maximum lift coefficient c_{Lmax}, Strouhal number St and pressure difference $\Delta P(t)$ at $t = t_0 + 1/2f$. The initial data ($t = t_0$) should correspond to the flow state with c_{Lmax}.

c) Test case 2D-3 (unsteady):

The inflow condition is

$$U(0, y, t) = 4U_m y(H - y)\sin(\pi t/8)/H^2,\ V = 0$$

with $U_m = 1.5\,\mathrm{m/s}$, and the time interval is $0 \le t \le 8\,\mathrm{s}$. This gives a time varying Reynolds number between $0 \le Re(t) \le 100$. The initial data ($t = 0$) are $U = V = P = 0$. The following quantities should be computed: drag coefficient c_D, lift coefficient c_L and pressure difference ΔP as functions of time for $0 \le t \le 8\,\mathrm{s}$, maximum drag coefficient c_{Dmax}, maximum lift coefficient c_{Lmax}, pressure difference $\Delta P(t)$ at $t = 8\,\mathrm{s}$.

2.3 3D Cases

For the 3D test cases the flows around a cylinder with square and circular cross–sections are considered. The problem configurations and boundary conditions are illustrated in Figs. 2 and 3. The outflow condition can be selected by the user. Some definitions are

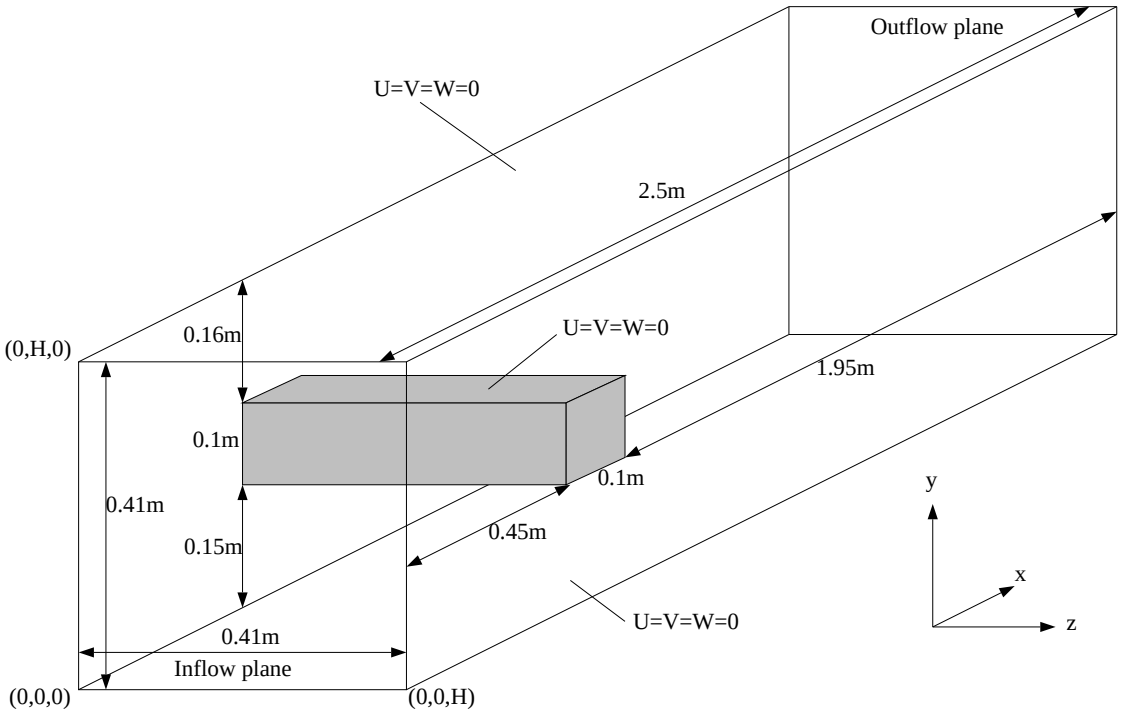

Figure 2: *Configuration and boundary conditions for flow around a cylinder with square cross–section.*

introduced to specify the values which have to be computed. The height and width of the channel is $H = 0.41\,\mathrm{m}$, and the side length and diameter of the cylinder are $D = 0.1\,\mathrm{m}$. The characteristic velocity is $\overline{U}(t) = 4U(0, H/2, H/2, t)/9$, and the Reynolds number is defined by $Re = \overline{U}D/\nu$. The drag and lift forces are

$$F_D = \int_S (\rho\nu \frac{\partial v_t}{\partial n} n_y - p n_x)\, dS \quad , \quad F_L = -\int_S (\rho\nu \frac{\partial v_t}{\partial n} n_x + P n_y)\, dS$$

with the following notations: surface of cylinder S, normal vector n on S with x-component n_x and y-component n_y, tangential velocity v_t on S and tangent vector $t = (n_y, -n_x, 0)$. The drag and lift coefficients are

$$c_D = \frac{2F_w}{\rho\overline{U}^2 DH} \quad , \quad c_L = \frac{2F_a}{\rho\overline{U}^2 DH}$$

The Strouhal number is $St = Df/\overline{U}$ with the frequency of separation f, and a pressure difference is defined by $\Delta P = \Delta P(t) = P(x_a, y_a, z_a, t) - P(x_e, y_e, z_e, t)$ with coordinates $(x_a, y_a, z_a) = (0.45, 0.20, 0.205)$ and $(x_e, y_e, z_e) = (0.55, 0.20, 0.205)$.

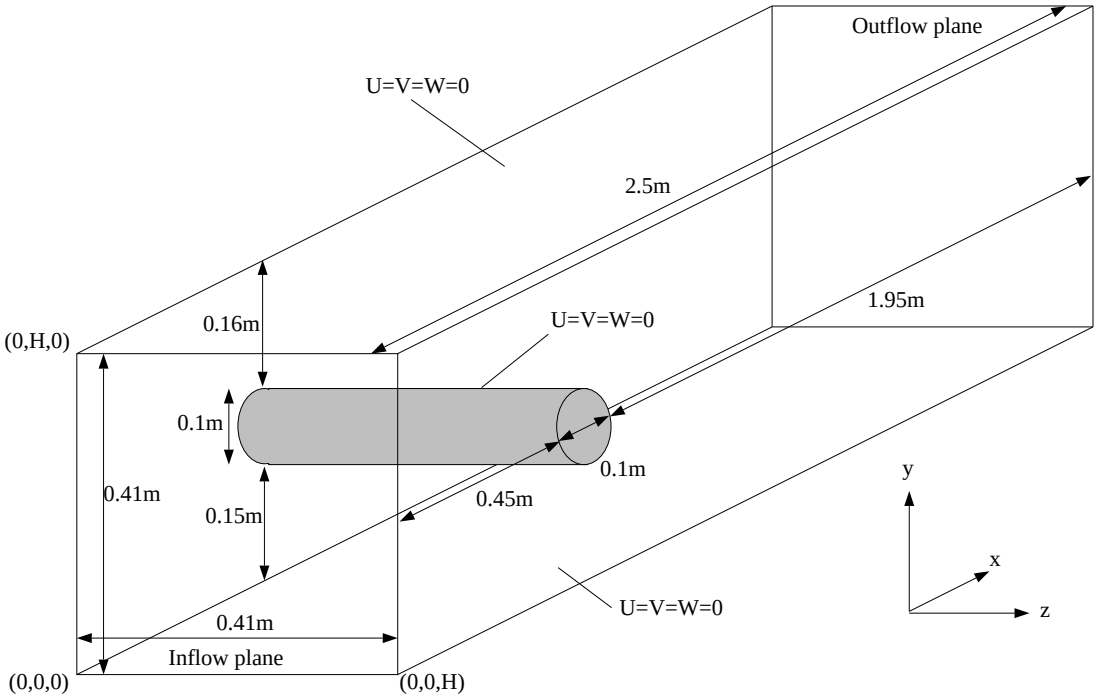

Figure 3: *Configuration and boundary conditions for flow around a cylinder with circular cross–section.*

a) Test cases 3D-1Q and 3D-1Z (steady):

The inflow condition is

$$U(0, y, z) = 16U_m yz(H - y)(H - z)/H^4,\ V = W = 0$$

with $U_m = 0.45\,\mathrm{m/s}$, yielding the Reynolds number $Re = 20$. The following quantities should be computed: drag coefficient c_D, lift coefficient c_L and pressure difference ΔP.

b) Test cases 3D-2Q and 3D-2Z (unsteady):

The inflow condition is

$$U(0, y, z, t) = 16U_m yz(H - y)(H - z)/H^4,\ V = W = 0$$

with $U_m = 2.25\,\mathrm{m/s}$, yielding the Reynolds number $Re = 100$. The following quantities should be computed: drag coefficient c_D, lift coefficient c_L and pressure difference ΔP as functions of time for <u>three</u> periods $[t_0, t_0 + 3/f]$ (with $f = f(c_L)$), maximum drag coefficient c_{Dmax}, maximum lift coefficient c_{Lmax} and Strouhal number St. The initial data ($t = t_0$) are arbitrary, however, for fully developed flow.

c) Test cases 3D-3Q and 3D-3Z (unsteady):

The inflow condition is

$$U(0, y, z, t) = 16U_m yz(H - y)(H - z)\sin(\pi t/8)/H^4,\ V = W = 0$$

with $U_m = 2.25\,\mathrm{m/s}$. The time interval is $0 \leq t \leq 8\,\mathrm{s}$. This yields a time-varying Reynolds number between $0 \leq Re(t) \leq 100$. The initial data ($t = 0$) are $U = V = P = 0$. The following quantities should be computed: drag coefficient c_D, lift coefficient c_L and pressure difference ΔP as functions of time for $0 \leq t \leq 8\,\mathrm{s}$, maximum drag coefficient c_{Dmax}, maximum lift coefficient c_{Lmax} and pressure difference $\Delta P(t)$ for $t = 8\,\mathrm{s}$.

2.4 Instructions for Computations

The following additional instructions concerning the computations were given to the participants:

- In the case of the steady calculations 2D-1, 3D-1Q and 3D-1Z, the results have to be presented for three successively coarsened meshes (notation: h_1, h_2 and h_3 with finest level h_1).
- Any iterative process used for the steady computations should start from zero values.
- In the case of the unsteady calculations 2D-2, 2D-3, 3D-2Q, 3D-2Z, 3D-3Q and 3D-3Z, the results have to be presented for three successively coarsened meshes (notation as in the steady case) with a finest time discretization (notation: Δt_1) and also for two successively coarsened time discretizations (notation: Δt_2 and Δt_3) together with the finest mesh h_1.
- The finest spatial mesh h_1, the finest time discretization Δt_1 and the coarsening strategies can be chosen by the user.
- The convergence criteria for the iterative method in the steady case and for each time step in the unsteady cases (in connection with implicit methods) can be chosen by the user.
- The outflow condition can be chosen by the user.
- If possible, the calculations should be performed on a workstation. For all computers used, the theoretical peak performance and the MFlop rate for the *LINPACK1000-benchmark* (in 64-bit arithmetic) should be provided. The LINPACK1000 value should be obtained with the same compiler options as used for the flow solver.
- In addition to the benchmark results a description of the solution methods should be given.

3. PARTICIPATING GROUPS AND NUMERICAL APPROACHES

In Table 1 the different groups that provided results for the present benchmark computation are listed, and the individual test cases for which results were provided are also indicated. In Table 2 the numerical methods and implementations of the participating groups are summarized. Only the major features which are the most important for the evaluation of the results are given. The following abbreviations are used in the table: Finite difference method (FD), Finite volume method (FV), Finite element method (FE), Navier-Stokes equations (NS) and Multigrid method (MG). PEAK means the peak performance in MFlops and LINP the Linpack1000 MFlop-rate.

Table 1: *Participating groups and test cases for which results were provided. The p indicates that only parts of the required results for the corresponding test case were given, and x indicates a full set of results*

Participants/test cases	2D			3D					
	1	2	3	1Q	1Z	2Q	2Z	3Q	3Z
1) RWTH Aachen, Aerodynamisches Institut *E. Krause, M. Weimer, M. Meinke*	x	x	x	x	x		p	p	p
2) ASC GmbH (TASCflow) *F. Menter, G. Scheuerer*					x				
3) TU Berlin Inst. für Strömungsmechanik *F. Thiele, L. Xue*	p	p	p	p	p	p	p	p	p
4) TU Chemnitz, Fakultät für Mathematik *A. Meyer, S. Meinel, U. Groh, M. Pester*	x	x	x						
5) Daimler-Benz AG (STAR-CD) *F. Klimetzek*				p					
6) Univ. Duisburg, Inst. für Verbrennung und Gasdyn. *D. Hänel, O. Filippova*	x	x	p	p	p	p	p	p	p
7) Univ. Erlangen, Lehrstuhl für Strömungsmechanik *F. Durst, M. Schäfer, K. Wechsler*	x	x	x	x	x		x		x
8) Univ. Freiburg, Inst. für Angewandte Mathematik *E. Bänsch, M. Schrul*	x	x	x	x	x			p	p
9) Univ. Hamburg, Inst. für Schiffbau *M. Perić, S. Muzaferija, V. Seidl*	x	x	x		x		p		
10) Univ. Heidelberg, Inst. für Angewandte Mathematik *R. Rannacher, S. Turek*	x	x	x	x	x	x	x	x	x
11) TU Karlsruhe, Inst. für Hydromechanik *W. Rodi, M. Pourquie*				x				p	
12) Univ. Karlsruhe, Inst. für Therm. Strömungsmasch. *C.-H. Rexroth, S. Wittig*	x								
13) Kyoto Inst. of Tech., Dept. of Mech. and Syst. Eng. *N. Satofuka, H. Tokunaga, H. Hosomi*	x	x							
14) Univ. Magdeburg, Inst. für Analysis und Numerik *L. Tobiska, V. John, U. Risch, F. Schieweck*	x		x						
15) TU München, Inst. für Informatik *C. Zenger, M. Griebel, R. Kreißl, M. Rykaschewski*	x	x	x	x		p		p	
16) UBW München, Inst. f. Strömungsmech. u. Aerodyn. *H. Wengle, M. Manhart*				x		p			
17) Univ. Stuttgart, Inst. für Computeranwendungen *G. Wittum, H. Rentz-Reichert*	x								

Table 2: *Numerical methods and implementation of participating groups*

	Space discretization	Time discretization	Solver	Implementation
1	FD, blockstructured non-staggered QUICK upwinding	fully implicit 2nd ord. equidistant	artificial compressibility expl. 5-step Runge-Kutta FAS-MG (steady) line-Jacobi (unsteady)	serial Fujitsu VPP500 1600 PEAK
2	FV, blockstructured 2nd ord. upwindig	implicit Euler equidistant	ILU with algebraic MG for linear problems	serial IBM RS6000/370 37 LINP
3	FV, blockstructured non-staggered QUICK upwinding	fully implicit 2nd ord. equidistant	stream function form fixed-point iteration ILU for lin. subproblems	serial SGI-Indigo2 75 PEAK parallel Cray T3D/16 16x88 LINP
4	FE, blockstructured 4Q1-Q1 BTD stabilisation	Projection 2 (Gresho) Crank-Nicolson (diff.) explicit Euler (conv.) adaptive	pseudo time step (steady) PCG for lin. subproblems hierarch. preconditioning	parallel GC/PP32 32x13.9 LINP
5a	FV, unstructured 1st ord. upwind	STARCD software	pressure correction	serial HP 735 13 LINP
5b	FV, unstructured CDS	STARCD software	pressure correction	serial HP 735 13 LINP
6	Lattice BGK equidistant orth. grid	explicit equidistant	gaskinetic solution of BGK-Boltzmann equation evol. of distribution funct.	serial HP735 13 LINP
7a	FV, blockstructured non-staggered CDS with def. corr.	Crank-Nicolson equidistant	nonlinear MG SIMPLE smoothing ILU for lin. subproblems	serial HP735 13 LINP
7b	FV, blockstructured non-staggered CDS with def. corr.	fully implicit 2nd ord. equidistant	nonlinear MG SIMPLE smoothing ILU for lin. subproblems	parallel GC/PP128,32,8 128x13.9 LINP
8a	FE, unstructured P2-P1 (Taylor-Hood) CDS	2nd order fract. step operator splitting equidistant	nonlinear GMRES PCG for lin. subproblems	serial SGI R4000 8.3 LINP
8b	FE, unstructured P2-P1 (Taylor-Hood) CDS adaptive refinement	2nd order fract. step operator splitting equidistant	nonlinear GMRES PCG for lin. subproblems	serial SGI R4400 13.2 LINP IBM RS6000/590 58 LINP
9a	FV, blockstructured CDS	fully implicit 2nd ord. equidistant	SIMPLE ILU for lin. subproblems	serial IBM RS6000/250 34 LINP
9b	FV, unstructured CDS	fully implicit 2nd ord. equidistant	SIMPLE ILU-CGSTAB for lin. subproblems	serial IBM RS6000/590 90 LINP

Table 2: *(continued)*

	Space discretization	Time discretization	Solver	Implementation
10	FE, blockstructured Q1(rot)-Q0 adaptive upwind	2nd order fract. step projection method adaptive	fixed-point iteration MG for lin. NS with Vanka smoother (steady) MG for scalar lin. subproblems (unsteady)	serial IBM RS6000/590 90 LINP
11	FV, structured CDS with momentum interpolation	explicit 3rd ord. Runge-Kutta equidistant	SIMPLE ILU for lin. subprobl.	serial SNI S600/20 5000 PEAK
12	FV, unstructured non-staggered adapt. 2nd ord. DISC deferred correction	–	SIMPLEC ILU-BICGSTAB for lin. subproblems	serial SUN SS10 5.5 LINP
13a	FD, structured	explicit Euler equidistant	stream function form pseudo time step SOR for lin. subprobl.	serial IBM RS6000/590 90 LINP
13b	FD, structured	explicit 4th order Runge-Kutta-Gill equidistant	stream function form SOR for lin. subprobl.	serial IBM RS6000/590 90 LINP
14a	FE, blockstructured P1-P0 (Crouzeix-Raviart) 1st order upwind	–	nonlinear MG Vanka smoother	serial HP737/125 6.6 LINP
14b	FE, blockstructured Q1(rot)-Q0 1st order upwind		fixed-point iteration MG for lin. NS with Vanka smoother	parallel GC/PP96 96x13.9 LINP
14c	FE, unstructured P1-P0 (Cr.-Rav.) Samarskij upwind adaptive refinement	BDF(2), equidistant	fixed-point iteration GMRES for pressure Schur-complement lin. MG for velocity	parallel GC/PP24 24x13.9 LINP
15a	FD, structured staggered, orthogonal CDS/UDS flux-blend.	explicit Euler adaptive	SOR for pressure	serial HP720 7.4 LINP
15b	FD, structured staggered, orthogonal CDS/UDS flux blend.	explicit Euler adaptive	SOR for pressure	parallel HP720 cluster 8x7.4 LINP
16	FV, blockstructured CDS	explicit 2nd ord. leap-frog time-lagged diff.	pressure correction Gauss-Seidel for lin. subproblems	serial SGI Indigo 9.6 LINP Convex C3820 19.2 LINP
17	FV, unstructured adaptive upwind	–	fixed-point iteration MG for lin. NS BILU$_\beta$ smoother	serial SGI R4400 8.3 LINP

4. RESULTS

The results of the benchmark computations are summarized in Tables 3-11. The number in the first column refers to the methods given in Table 2. The last column contains the performance of the computer used (as given by the contributors), either the Linpack1000 Mflop rate (LINP) or the peak performance (PEAK), which of course should be taken into account when comparing the different computing times. The column "unknowns" refers to the total number, i.e. the sum of unknowns for all velocity components and pressure. The CPU timings are all given in seconds. In the last row of each table estimated intervals for the "exact" results are indicated (as suggested by the authors on the basis of the obtained solutions).

We remark that for the 2D time-periodic test case 2D-2 also measurements were carried out, where the Strouhal number and time-averaged velocity profiles at different locations along the channel are determined experimentally. However, a direct comparison with the numerical results in Table 4 is problematic, because owing to the short distance between the inlet and the cylinder for the computations, the flow conditions in front of the cylinder are slightly different. To give some comparison with method 7a (see Table 2), a computation with a longer distance between the inlet and cylinder was carried out. The experimentally obtained Strouhal number of $St = 0.287 \pm 0.003$ agrees very well with the numerically computed value of $St = 0.289$. A comparison of time-averaged velocity profiles can be seen in Fig. 4, which also are in fairly good agreement.

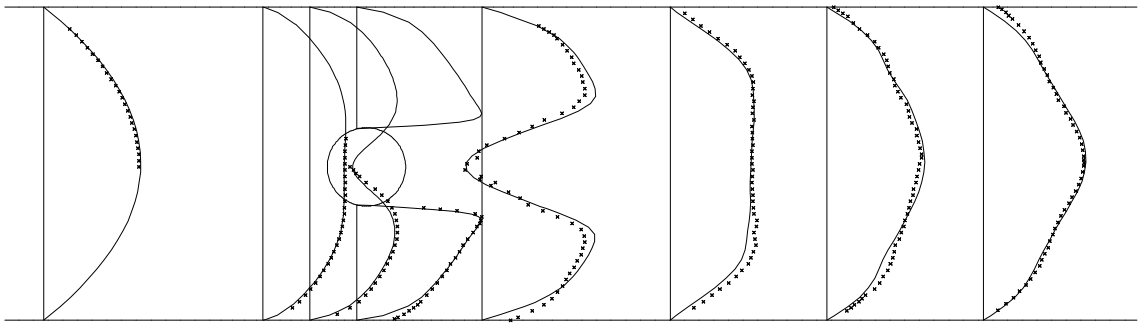

Figure 4: *Comparison of experimental and numerical time-averaged velocity profiles for test case 2D-2 with extended inlet part.*

Table 3: *Results for steady test case 2D-1*

	Unknowns	c_D	c_L	L_a	ΔP	Mem.	CPU time	MFlop rate
1	200607	5.5567	0.0106	0.0845	0.1172	15	788	1600 PEAK
	51159	5.5567	0.0106	0.0843	0.1172	4	273	
	13299	5.5661	0.0105	0.0835	0.1169	1	144	
3a	10800	5.6000	0.0120	0.0720	0.1180	2.5	121	75 PEAK
4	297472	5.5678	0.0105	0.0847	0.1179	137	31000	445 LINP
	75008	5.5606	0.0107	0.0849	0.1184	73	8000	
	19008	5.5528	0.0118	0.0857	0.1199	57	2000	
6	1314720	5.8190	0.0110	0.0870	0.1230	40	80374	13 LINP
	332640	5.7740	0.0030	0.0830	0.1230	10	10461	
	85140	5.7890	-0.0060	0.0870	0.1230	2.6	1262	
7a	294912	5.5846	0.0106	0.0846	0.1176	75	192	13 LINP
	73728	5.5852	0.0105	0.0845	0.1176	19	47	
	18432	5.5755	0.0102	0.0842	0.1175	5	13	
8a	20487	5.5760	0.0110	0.0848	0.1170	9.0	2574	8.3 LINP
	6297	5.5710	0.0130	0.0846	0.1160	2.9	362	
	2298	5.4450	0.0200	0.0810	0.1110	1.3	109	
9a	240000	5.5803	0.0106	0.0847	0.1175	53	9200	34 LINP
	60000	5.5786	0.0106	0.0847	0.1173	10	1400	
	15000	5.5612	0.0109	0.0848	0.1166	2.5	200	
10	2665728	5.5755	0.0106	0.0780	0.1173	350	677	90 LINP
	667264	5.5718	0.0105	0.0770	0.1169	89	169	
	167232	5.5657	0.0102	0.0730	0.1161	22	52	
	42016	5.5608	0.0091	0.0660	0.1139	5	18	
12	32592	5.5069	0.0132	0.0830	0.1155	18	1796	5.5 LINP
	26970	5.5125	0.0056	0.0827	0.1154	15	1099	
	22212	5.6026	-0.0031	0.0815	0.1167	13	3437	
13a	25410	5.6145	0.0159	0.8315	3.0002	4	14203	90 LINP
	12738	5.6114	0.0169	0.8224	2.9943	2	3018	
	6562	5.7377	0.0514	0.8107	3.2277	1		
14a	3077504	5.6323	0.0137	0.0782	0.1159	214	15300	6.6 LINP
	768704	5.6382	0.0102	0.0775	0.1156	53	5490	
	191840	5.5919	-0.0009	0.0750	0.1143	13	2800	
14b	30775296	5.5902	0.0108	0.0853	0.1174	5340	1534	1334 LINP
	7695104	5.6010	0.0110	0.0844	0.1174	1341	400	
	1922432	5.6227	0.0113	0.0833	0.1172	338	119	
14c	797010	5.5708	0.0167	0.0837	0.1168	460	8000	334 LINP
	363457	5.5598	0.0142	0.0835	0.1166	230	3290	
	176396	5.5106	0.0046	0.0835	0.1150	110	2560	
15a	432960	5.5602	0.0329	0.0730	0.1054	4.4	179986	7.4 LINP
	108240	5.6300	0.0751	0.0720	0.1037	1.1	13593	
	27060	5.7769	0.2085	0.0680	0.0998	0.3	688	
17	111342	5.5610	0.0107		0.1170	87	2568	8.3 LINP
	60804	5.5520	0.0102		0.1168	47	1092	
	19416	5.5160	0.0099		0.1158	15	373	
	lower bound	5.5700	0.0104	0.0842	0.1172			
	upper bound	5.5900	0.0110	0.0852	0.1176			

Table 4: *Results for time–periodic test case 2D-2*

	Unknowns								
	Space	Time	c_{Dmax}	c_{Lmax}	St	ΔP	Mem.	CPU time	MFlop rate
1	267476	67	3.2224	0.9672	0.2995	2.4814	—	—	1600 PEAK
	267476	34	3.2030	0.9223	0.2941	2.4664	—	—	
	267476	18	3.1605	0.8026	0.2901	2.4466	—	—	
	68212	67	3.2171	0.9591	0.2995	2.5009	—	—	
	17732	68	3.2168	0.9295	0.2979	2.5573	—	—	
3	12800	34	3.2200	0.9720	0.2960	2.4700	2.5	789	75 PEAK
4	297472	670	3.2460	0.9840	0.2985	2.4900	137	6600	445 LINP
	297472	338	3.2710	0.9800	0.2959	2.4870	137	3400	
	297472	172	3.3200	0.9720	0.2907	2.4810	137	1700	
	75008	670	3.2410	0.9910	0.2985	2.5020	73	2350	
	19008	674	3.2320	1.0260	0.2967	2.5320	57	1350	
6	332640	12000	4.1210	1.6120	0.3330	3.1420	10	10086	13 LINP
	85140	6000	4.7330	2.0600	0.3380	3.4300	2.6	1259	
7a	294912	36	3.2358	1.0069	0.3003	2.4892	75	6167	13 LINP
	294912	19	3.2356	1.0000	0.2973	2.4871	75	6391	
	294912	10	3.2152	0.9028	0.2881	2.4715	75	4994	
	73728	36	3.2443	1.0261	0.2994	2.4929	19	1946	
	18432	36	3.2706	1.0695	0.2968	2.5035	5	445	
8a	29084	66	3.2240	1.0060	0.3020	2.4860	11	4992	8.3 LINP
	29084	33	3.2470	1.0740	0.3030	2.5010	11	3777	
	29084	16	3.2900	1.2500	0.3130	2.5700	11	3217	
	8764	66	3.1740	0.9640	0.3000	2.4630	3.6	1000	
	2978	70	2.8920	0.5540	0.2890	2.2870	1.5	339	
9a	240000	5000	3.2267	0.9862	0.3017	2.4833	53	32500	34 LINP
	60000	10000	3.2232	0.9830	0.3012	2.4773	10	8550	
	60000	5000	3.2232	0.9832	0.3012	2.4773	10	4500	
	60000	2500	3.2232	0.9836	0.3012	2.4773	10	3400	
	15000	5000	3.2058	0.9651	0.2994	2.4587	2.5	3240	
10	667264	612	3.2314	0.9999	0.2973	2.4707	128	8545	90 LINP
	667264	204	3.2351	1.0123	0.2957	2.4734	128	2850	
	667264	68	3.2771	1.1205	0.2997	2.4961	128	1065	
	167232	188	3.2498	1.0081	0.2927	2.4410	32	655	
	42016	164	3.2970	0.8492	0.2713	2.3423	8	147	
13b	25410	6755	3.1822	1.0692	0.2960	2.6066	5.1	44710	90 LINP
	25410	3877	3.1895	1.0883	0.2968	2.6057	4.8	27175	
	25410	1678	3.2043	1.1268	0.2979	2.5307	4.7		
	12738	6799	3.1945	1.1233	0.2941	2.6140	2.9	13045	
	6562	7223	3.1317	1.2961	0.2768	3.0253	1.8		
15a	432960	7790	3.0804	0.7256	0.2778	2.1330	4.4	108844	7.4 LINP
	108240	4003	3.1677	0.6880	0.2646	2.0954	1.1	34876	
	108240	3859	3.1096	0.8249	0.2841	2.1105	1.1	58003	
	27060	1985	3.2544	0.5658	0.2336	1.9727	0.3	3796	
	27060	1670	3.1759	0.7656	0.2740	1.9961	0.3	4188	
	lower bound		3.2200	0.9900	0.2950	2.4600			
	upper bound		3.2400	1.0100	0.3050	2.5000			

Table 5: *Results for unsteady test case 2D-3*

	Unknowns							
	Space	Time	c_{Dmax}	c_{Lmax}	ΔP	Mem.	CPU time	MFlop rate
1	267476	400	2.9387	0.3504	-0.1048	—	—	1600 PEAK
	68212	800	2.9459	0.4492	-0.1057	—	—	
	17732	800	2.9532	0.3908	-0.1007	—	—	
3	12800	800	2.9600	0.4300	-0.0976	2.5	7567	75 PEAK
4	297472	16000	2.9715	0.4806	-0.1101	137	160000	445 LINP
	297472	8000	2.9984	0.4794	-0.1035	137	88000	
	297472	4000	3.0508	0.4750	-0.1018	137	48000	
	75008	16000	2.9660	0.4903	-0.1098	73	47000	
	19008	16000	2.9551	0.5228	-0.1061	57	31000	
6	332640	36960	3.8420	1.1100	0.0200	10	19772	13 LINP
	85140	9460	4.5310	1.7610	0.0090	2.6	2511	
7a	294912	800	2.9520	0.4793	-0.1086	75	43119	13 LINP
	294912	400	2.9520	0.4787	-0.1016	75	29165	
	294912	200	2.9512	0.4021	-0.1047	75	22141	
	73728	800	2.9511	0.4711	-0.0995	19	10003	
	18432	800	2.9461	0.4638	-0.1024	5	2847	
8a	21508	1600	2.9200	0.4910	-0.1110	8	44028	8.3 LINP
	21508	800	2.9210	0.5390	-0.1140	8	31481	
	21508	400	2.9230	0.7250	-0.1160	8	25512	
	5822	1600	2.8160	0.3560	-0.1060	2.5	9294	
	1705	1600	2.7220	0.0055	-0.1220	1.1	2109	
9a	240000	5000	2.9505	0.4539	-0.1095	53	220000	34 LINP
	60000	10000	2.9483	0.4651	-0.1062	10	92000	
	60000	5000	2.9483	0.4630	-0.1062	10	64000	
	60000	2500	2.9482	0.4575	-0.1039	10	38000	
	15000	5000	2.9397	0.4349	-0.1095	2.5	22000	
10	667264	4540	2.9538	0.4782	-0.1053	128	62734	90 LINP
	667264	1612	2.9566	0.5533	-0.1029	128	22431	
	667264	704	3.0650	0.8443	-0.1090	128	11832	
	167232	4068	2.9776	0.4768	-0.1097	32	14005	
	42016	2908	3.0949	0.3223	-0.0951	8	2532	
14c	638880	800	3.0599	0.6326	-0.1100	550	740000	334 LINP
	858848	800	3.1441	0.5266	-0.1142	850	660000	668 LINP
15a	432960	9060	2.8916	0.2649	-0.0987	4.4	237397	7.4 LINP
	108240	4070	2.8927	0.3171	-0.0956	1.1	29140	
	108240	4020	3.0134	0.2921	-0.0945	1.1	25697	
	27060	2857	3.1817	0.2702	-0.1138	0.3	3371	
	27060	2013	3.0098	0.3973	-0.0941	0.3	2541	
	lower bound		2.9300	0.4700	-0.1150			
	upper bound		2.9700	0.4900	-0.1050			

Table 6: *Results for steady test case 3D-1Q*

	Unknowns	c_D	c_L	ΔP	Mem.	CPU time	MFlop rate
1	2530836	7.6415	0.0673	0.1740	251	1975	5000 PEAK
	657492	7.6029	0.0665	0.1738	72	702	1600 PEAK
3	634872	7.6100	0.0642	0.1730	72	1935	1408 LINP
5a	1472000	7.9200	0.0645	0.1751	121	127984	13 LINP
	184000	8.0400	0.0642	0.1722	17	3805	
	23000	7.6600	0.0720	0.1609	3	73	
5b	1472000	7.4400	0.0615	0.1721			
	184000	7.2800	0.0582	0.1673			
	23000	6.7400	0.0615	0.1509			
6	6303750	8.0930	0.0700		43	168657	13 LINP
7a	454656	7.5395	0.0797	0.1715	115	9525	13 LINP
	56832	7.1280	0.0861	0.1616	13	1280	
	7104	6.4590	0.0988	0.1385	3	88	
8a	362613	7.6480	0.0670	0.1751	126	46970	13.2 LINP
	73262	7.6530	0.0590	0.1766	28	6590	
8b	97822	7.6340	0.0660	0.1742	38	8648	13.2 LINP
10	6094976	7.6148	0.0600	0.1729	690	8244	90 LINP
	768544	7.5622	0.0503	0.1683	88	1267	
	97736	7.3069	0.0348	0.1590	10	380	
11	1425600	7.7583	0.0511	0.1744	100	2538	5000 PEAK
	460800	7.7673	0.0406	0.1721	38	536	
	128000	7.2372	0.0602	0.1611	17	86	
15b	6724000	6.0770	0.0859	0.0825	64	10600	52 LINP
	1681000	5.5060	0.1420	0.0796	16	1400	
16	2007040	7.3700	0.0619	0.1720	25	45000	19.2 LINP
	405503	7.2500	0.0549	0.1680	6	11000	9.6 LINP
	lower bound	7.5000	0.0600	0.1720			
	upper bound	7.7000	0.0800	0.1800			

Table 7: *Results for steady test case 3D-1Z*

	Unknowns	c_D	c_L	ΔP	Mem.	CPU time	MFlop rate
1	2426292	6.1295	0.0093	0.1693	233	2097	5000 PEAK
	630564	6.1230	0.0095	0.1680	71	1238	1600 PEAK
2	555000	6.1440	0.0074	0.1604	122	8731	26 LINP
	276800	5.8600	0.0042	0.1616	67	6094	
3	608496	6.1600	0.0095	0.1690	74	4150	1408 LINP
6	6303750	6.2330	-0.0040		43	221706	13 LINP
7b	12582912	6.1932	0.0093	0.1709	3571	2630	1779 LINP
	1572864	6.1868	0.0092	0.1703	518	1120	445 LINP
	196608	6.1366	0.0098	0.1673	71	460	111 LINP
8a	362613	6.1430	0.0084	0.1694	126	51280	13.2 LINP
	73262	6.0990	0.0067	0.1695	28	7178	
9	2355712	6.1800	-0.0010	0.1691		62000	90 LINP
	753664	6.1720	0.0090	0.1680		6000	
	94208	6.1310	0.0100	0.1605		950	
10	6116608	6.1043	0.0079	0.1672	700	8440	90 LINP
	771392	5.9731	0.0059	0.1605	89	1466	
	98128	5.8431	0.0061	0.1482	11	290	
	lower bound	6.0500	0.0080	0.1650			
	upper bound	6.2500	0.0100	0.1750			

Table 8: *Results for time–periodic test case 3D-2Q*

	Unknowns		c_{Dmax}	c_{Lmax}	St	Mem.	CPU time	MFlop rate
	Space	Time						
3	634872	188	4.3170	0.0495	0.3130	74	3368	1408 LINP
	634872	95	4.3170	0.0495	0.3210	74	2754	
6	6303750	18000	4.5870	-0.0050	–	43	168657	13 LINP
10	6094976	142	4.3923	0.0146	0.2777	840	29428	90 LINP
	6094976	124	4.3932	0.0191	0.2806	840	29945	
	6094976	84	4.4071	0.0896	0.2400	840	30372	
	768544	–	4.4819	0.0036	–	105	–	
	97736	–	4.5529	-0.0080	–	13	–	
16	2007040	1726	4.6738	0.0389	0.3488	25	20040	19.2 LINP
	405503	833	4.8808	0.0392	0.3610	6	10020	9.6 LINP
	lower bound		?	?	?			
	upper bound		?	?	?			

Table 9: *Results for time–periodic test case 3D-2Z*

	Unknowns							
	Space	Time	c_{Dmax}	c_{Lmax}	St	Mem.	CPU time	MFlop rate
1	630564	177	3.3018	-0.0014	0.3390	78	26115	1600 PEAK
3	608496	–	3.2250	-0.0142	–	74		1408 LINP
	608496	–	3.2250	-0.0142	–			
6	6303750	18000	3.7920	-0.0210	–	43	142646	13 LINP
7b	12582912	93	3.3052	-0.0105	0.3409	3571	24459	1779 LINP
	1572864	378	3.3057	-0.0118	0.3172	518	9487	445 LINP
	1572864	261	3.3054	-0.0118	0.2250	518	2740	445 LINP
	1572864	126	3.3050	-0.0018	0.2400	518	1956	445 LINP
	196608	–	3.3121	-0.0150	–	71	–	111 LINP
9b	2355712		3.2968					90 LINP
	753664		3.3254					
	94208		3.3284					
10	6116608	128	3.2950	-0.0081	0.2912	840	31145	90 LINP
	6116608	120	3.2970	-0.0025	0.2830	840	31730	
	6116608	80	3.3200	0.0480	0.2684	840	21586	
	771392	68	3.3801	0.0086	0.2343	105	2163	
	98128	–	3.4593	-0.0102	–	13	–	
	lower bound		3.2900	-0.0110	0.2900			
	upper bound		3.3100	-0.0080	0.3500			

Table 10: *Results for unsteady test case 3D-3Q*

	Unknowns							
	Space	Time	c_{Dmax}	c_{Lmax}	ΔP	Mem.	CPU time	MFlop rate
1	657492	800	4.3804	0.0308	-0.1392	78	121960	1600 PEAK
3	634872	1600	4.3030	0.0476	-0.1361	74	51253	1408 LINP
	634872	800	4.3020	0.0473	-0.1354	74	37241	
6	6303750	18000	4.8680	0.0310		43	168657	13 LINP
8a	362613	1000	4.5530	0.0137	-0.1436	126	398000	58 LINP
8b	228451	1000	4.5080	0.0432	-0.1427	105	915000	13.2 LINP
10	6094976	772	4.4086	0.0133	-0.1264	840	164749	90 LINP
	6094976	392	4.5698	0.0262	-0.1213	840	89679	
	6094976	82	5.5709	0.1230	0.0183	840	35600	
	768544	696	4.5223	0.0061	-0.1113	105	22747	
	97736	588	4.5820	0.0033	-0.0718	13	3031	
11	3712800	7720	4.3400	0.0500	-0.0810	105	5711	5000 PEAK
	1523200	7720	4.4000	0.0480	-0.1160	48	2741	
	352000	7720	4.3600	0.0680	-0.1090	18	706	
	lower bound		4.3000	0.0100	-0.1400			
	upper bound		4.5000	0.0500	-0.1200			

Table 11: *Results for unsteady test case 3D-3Z*

	Unknowns							
	Space	Time	c_{Dmax}	c_{Lmax}	ΔP	Mem.	CPU time	MFlop rate
1	630564	800	3.2826	0.0027	-0.1117	79	156460	1600 PEAK
3	608496	1600	3.2590	0.0026	-0.1072	74	76142	1408 LINP
	608496	800	3.2590	0.0026	-0.1157	74	50764	
6	6303750	18000	4.1600	0.0200		43	142646	13 LINP
7b	1572864	1600	3.3011	0.0026	-0.1102	518	149923	445 LINP
	1572864	800	3.3008	0.0026	-0.1105	518	93055	445 LINP
	1572864	400	3.3006	0.0026	-0.1107	518	62026	445 LINP
	196608	1600	3.3053	0.0028	-0.1066	71	63057	111 LINP
8a	362613	1000	3.2340	0.0028	-0.1114	126	347000	58 LINP
8b	199802	1000	3.2120	0.0122	-0.1112	105	846000	13.2 LINP
	98637	1000	3.2350	0.0123	-0.1114	39	243000	
10	6116608	668	3.2802	0.0034	-0.0959	840	164837	90 LINP
	6116608	272	3.3748	0.0360	-0.0603	840	77538	
	6116608	60	2.7312	0.0069	-0.0682	840	29742	
	771392	724	3.3323	0.0033	-0.0766	105	24745	
	98128	660	3.4200	0.0040	-0.0407	13	5687	
	lower bound		3.2000	0.0020	-0.0900			
	upper bound		3.3000	0.0040	-0.1100			

5. DISCUSSION OF RESULTS

On the basis of the results obtained by these benchmark computations some conclusions can be drawn. These have to be considered with care, as the provided results depend on parameters which are not available for the authors of this report, e.g., design of the grids, setting of stopping criteria, quality of implementation, etc.

For five of the ten questions above the answers seem to be clear:

1. In order to compute incompressible flows of the present type (laminar) accurately and efficiently, one should use implicit methods. The step size restriction enforced by explicit time stepping can render this approach highly inefficient, as the physical time scale may be much larger than the maximum possible time step in the explicit algorithm. This is obvious from the results for the stationary cases in 2D and 3D, and also for the nonstationary cases in 2D. For the nonstationary cases in 3D only too few results on apparently too coarse meshes have been provided, in order to draw clear conclusions. This question requires further investigation.

2. Flow solvers based on conventional iterative methods on the linear subproblems have on fine enough grids no chance against those employing suitable multigrid techniques. The use of multigrid can allow computations on workstations (provided the problem fits into the RAM) for which otherwise supercomputers would have to be used. In the submitted solutions supercomputers (Fujitsu, SNI, CRAY) have mainly been used for their high CPU power but not for their large storage capacities. For example, in test case 3D-3Z

(Table 11) the solutions 1 and 3 require with about 600,000 unknowns on supercomputers significantly more CPU time than the solution 10 with the same number of unknowns on a workstation.

3. The most efficient and accurate solutions are based either on finite element or finite volume discretizations on contour adapted grids.

4. The computation of steady solutions by pseudo time-stepping techniques is inefficient compared with using directly a quasi-Newton iteration as stationary solver.

5. For computing sensitive quantities such as drag and lift coefficients, higher order treatment of the convective term is indispensable. The use of only first order upwinding (or crude approximation of curved boundaries) does not lead to satisfactory accuracy even on very fine meshes (several million unknowns in 2D).

For the remaining five questions the answers are not so clear. More test calculations will be necessary to reach more decisive conclusions. The following preliminary interpretations of the results obtained so far may become the subject of further discussion:

6. In computing nonstationary solutions, the use of operator splitting (pressure correction) schemes tends to be superior to the more expensive fully coupled approach, but this may depend on the problem as well as the quantity to be calculated (compare, e.g., for the test case 2D-3 (Table 5), the solution 14c with 7a and 10). Further, as fully coupled methods also use iterative correction within each time step (possibly adaptively controlled), the distinction between fully coupled and operator splitting approach is not so clear.

7. The use of higher than second-order discretizations in space appears promising with respect to accuracy, but there remains the question of how to solve efficiently the resulting algebraic problems (see the results of 8 for all test cases). The results provided for this benchmark are too sparse to allow a definite answer.

8. The most efficient solutions in this benchmark have been obtained on blockwise structured grids which are particularly suited for multigrid algorithms. There is no indication that fully unstructured grids might be superior for this type of problem, particularly with respect to solution efficiency (compare the CPU times reported for the solutions 7 and 9 in 2D). The winners may be hierarchically structured grids which allow local adaptive mesh refinement together with optimal multigrid solution.

9. From the contributed solutions to this benchmark there is no indication that a-posteriori grid adaptation in space is superior to good hand-made grids (see the results of 14c). This, however, may drastically change in the future, particularly in 3D. Intensive development in this direction is currently in progress.
For nonstationary calculations, adaptive time step selection is advisible in order to achieve reliability and efficiency (see the results of 10).

10. The treatment of the nonlinearity by nonlinear multigrid has no clear advantage over the quasi-Newton iteration with multigrid for the linear subproblems (compare the results of 7 with those of 10). Again, it is the extensive use of well-tuned multigrid (wherever in the algorithm) which is decisive for the overall efficiency of the method.

6. CONCLUDING REMARKS

The authors would like to add some final remarks to the report presented. Although, this benchmark has been fairly successful as it has made possible some solidly based comparison between various solution approaches, it still needs further development. Particularly the following points are to be considered:

1. In the case 3D-3Z it should be the maximum absolute value of the lift which has to be computed as c_L may become negative.

2. In the nonstationary test cases further characteristic quantities (e.g., time averages, pressure values, etc.) should be computed, as in some cases, by chance, "maximum values" may be obtained with good accuracy even without capturing the general pattern of the flow at all.

3. For the nonstationary 3D problems a higher Reynolds number should be considered, since in the present case (Re = 100) the problem may be particularly hard as the flow tends to become almost stationary.

Even in the laminar case, the chosen nonstationary 3D problems showed to be harder than expected. In particular, it was apparently not possible to achieve reliable reference solutions for the test cases 3D-2Q and 3D-2Z. Hence the benchmark has to be considered as still open and everybody is invited to try again.

ACKNOWLEDGMENTS

The authors thank all members of the various groups who have contributed results for the benchmark computations, K. Wechsler for his help in evaluating the results and J. Jovanovic and M. Fischer for carrying out the experiments.